Study on the Hydrothermal Coupling Characteristics of Polyurethane Insulation Boards Slope Protection Structure Incorporating Phase Change Effect

Hailiang Liu
Jilin University
Donghe Ma
Water Northeastern Investigation Design and Research Co., Ltd.
Changming Wang (wangcm@jlu.edu.cn)
Jilin University
Xiaoyang Liu
Jilin University
Di Wu
Jilin University
Bailong Li
Jilin University
Kaleem Ullah Jan Khan
Jilin University

Research Article

Keywords: Anti-frost structure, Polyurethane insulation boards, Hydrothermal coupling, Phase change

Posted Date: May 27th, 2021

DOI: https://doi.org/10.21203/rs.3.rs-546799/v1

Study on the Hydrothermal Coupling Characteristics of Polyurethane Insulation Boards Slope Protection Structure Incorporating Phase Change Effect

Hailiang Liu[1], Donghe Ma[2], Changming Wang[1,*], Xiaoyang Liu[1], Di Wu[1], Bailong Li[1], Kaleem Ullah Jan Khan[1]

[1]College of Construction Engineering, Jilin University, Changchun 130012, China.

[2]Senior Engineer, China Water Northeastern Investigation Design and Research Co., Ltd., Changchun 130061, China.

* Corresponding author: wangcm@jlu.edu.cn

Abstract: As an important hydraulic infrastructure, the canals are essential for agricultural irrigation, shipping and industry. In the seasonal freeze regions, the water conveyance canals are damaged due to the effects of freeze-thaw cycles. The freeze depth of soil in the water transfer canal varies considerably due to changes in temperature and water content. The paper compares the relationship of the freeze depth, temperature and water content by field tests and numerical calculation methods Incorporating phase change. The results show that the decrease in temperature causes the water in the soil to freeze, the ice front migrate downwards, and the water in soil below ice front gradually migrate towards the ice front, resulting a large difference in water content of the soil before and after freezing. An insulation slope structure, Polyurethane insulation board + Concrete board slope structure (PC), is proposed in this paper to mitigate the effect of freezing and thawing on the water conveyance canals. Under the protective effect, the freeze depth decreases

significantly. In addition, this paper compares the anti-frost effect of different thicknesses polyurethane insulation boards, and the results can provide a reference for the anti-frost design of water conveyance canals.

Key words: Anti-frost structure; Polyurethane insulation boards; Hydrothermal coupling; Phase change;

1 Introduction

Frozen soil is widespread across the world, covering a total area of about 23% of the land area[1]. Different types of frozen soil cover the territory of China, of which the total area of seasonal frozen soil is about $4.76\times10^{6}km^{2}$, accounting for about 49.6% of China's territory[2]. As society develops, human engineering activities inevitably conducted in seasonal freeze regions. For example, to solve the drought problems in northern seasonal freeze regions, water transfer canals are usually built to transfer water from water-rich areas to arid areas. Under the influence of temperature, the soil in seasonal freeze regions shows the characteristics of "freezing and thawing". The water conveyance canals built in the seasonal freeze region are damaged by seepage and freeze-thaw, such as frost heave, hollow and collapse damage (Fig.1)[3]. For arid and cold regions where water resources are extremely scarce, frost damage to canals has become a shackle for the safe and efficient operation of water transfer projects and economic development[4-7].

Fig. 1 Frost damage to canals

Damage to canals in the seasonal freeze regions is influenced by the environment factors(solar radiation, air thermal convection, precipitation, evaporation, etc.), the properties of soil (permeability, water content, gradation, pore space, etc.), the water table, and the form of canals (section form and lining structure, etc.)[3]. The study of soil frost heave can be traced back to the formulation of the First and the Second Frost Heave Theories[8-11]. However, the theory of frost heave in this period was not further developed due to the constraints of experimental conditions and computational efficiency. Nevertheless, the development of the two theories of frost heave has contributed significantly to subsequent research on frost heave. Since 1980s, technological development made it possible for scholars from various countries to conduct experimental studies on frost heave, thus providing great convenience to study the interaction between temperature and water in soils[12,13]. Kunio and Yurie (2016)[14] established the relationship between the permeability coefficient and temperature, ice content of the soil by unsaturated soil permeability tests. In recent years, with the development of computing technology, numerical methods have been widely used in solving the freeze issues. Numerical calculations make it possible to simulate changes in temperature and water in the soil, providing a reference for actual projects[15-17]. Li and Lai et al[18] study the mechanism of frost heave in a water conveyance canal by numerical simulation, and the results showed that the soil frost damage was caused by freezing of water in the

soil. In addition, numerical analysis is equally effective in predicting the damage mechanism of lining structures, which provides a basis for the design of concrete lining protection[19]. In addition to theoretical studies and numerical simulations, the physical models are also important in the study of the freezing effect of soils[15-17]. Li and Liu et al[20] conducted a soil bag frost protection test to investigate the effect of soil bags, and their findings showed that soil bags were able to inhibit the migration of water significantly.

Although numerical calculations, as well as laboratory tests, have achieved numerous achievements in the study of the hydrothermal characteristics of water conveyance canals, the accuracy of the results is questioned at times due to the various assumptions and the boundary conditions. As for the laboratory model tests, although they provide a more realistic reflection of the effects of temperature and water on freeze, the physical model developed in the laboratory is unable to fulfil the temporal and dimensional effects that affect the freeze in the canals. Using just one method (laboratory tests or numerical simulations) is inadequate in determining the freezing characteristics of the canals. Therefore, this paper takes the main canal of the Hada Mountain Water Conservancy Project as an example and monitors the freeze depth and water change of the canal by field tests. Combined with the numerical simulation of hydrothermal coupling, this paper proposes the application of polyurethane insulation board for frost protection on the slope of water conveyance canals, which provides a reference for the design of frost protection.

2 Study area

The Hada Mountain Water Conservancy Project locates on the second mainstream of the Songhua River about 20km from the southeast of Songyuan City, Jilin Province, China (Fig. 2a,b).

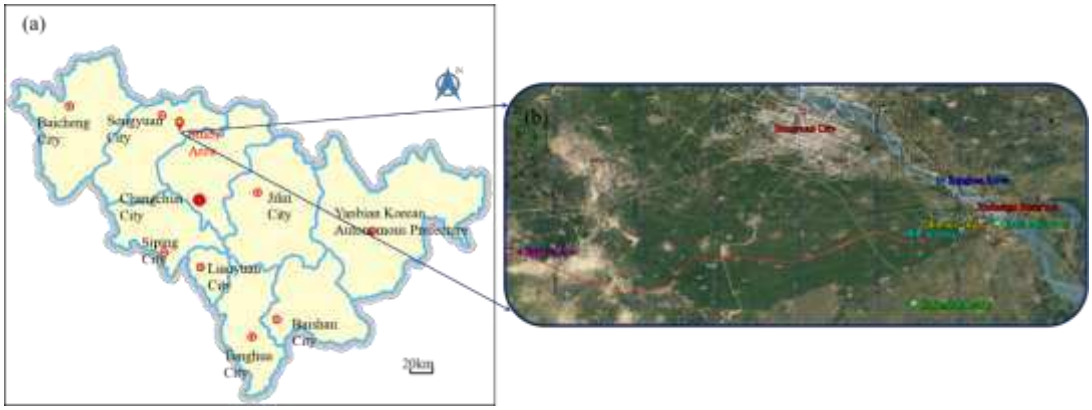

Fig. 2 Detailed overview of main canal of Hada Mountain Water Conservancy Project (a: Geographical location map of the study area; b: Satellite map of the study area, c: Soil slope, d: Insulation board and Concrete board slope protection)

According to the statistics of meteorological data from 1971 to 2012 (41 years) in Songyuan City, the average freeze period is 123 days per year, with the longest freeze period being 146 days and the shortest 102 days. Freezing has occurred from 22 October to 29 November, thawing has begun on 28 February to 31 March. An important index of coldness in a freeze-thaw cycle is the Freezing Index, which is cumulative of negative daily average temperature (°C) during a freezing period, which can be calculated according to Eq.1.

$$I_f = \int_{t_0}^{t_1} |T| \, dt \, , \; T<0°C \tag{1}$$

Where: I_f is the Freezing Index (°C·d), t_0, t_1 are the first and last day of the year when the temperature is below 0°C (d), and T is the temperature (°C).

During the 1971-2011 period, the Freezing Index of Songyuan City is shown in Fig. 3a, with a maximum Freezing Index of 1999°C·d, a minimum Freezing Index of 1041°C·d and an average Freezing Index of 1443°C·d. According to the local weather data, the freeze and thaw cycle in 2011-2012 is approximately sinusoidal (Fig. 3b) and the Freeze Index for 2011-2012 is calculated as 1613°C·d according to Eq.1. According to previous Freezing Index, the degree of coldness in 2011-2012 was moderate.

$$T=-5+20\sin(2\pi t+\pi/2) \tag{2}$$

93 Where: T is the daily temperature (°C) and t is the time (d).

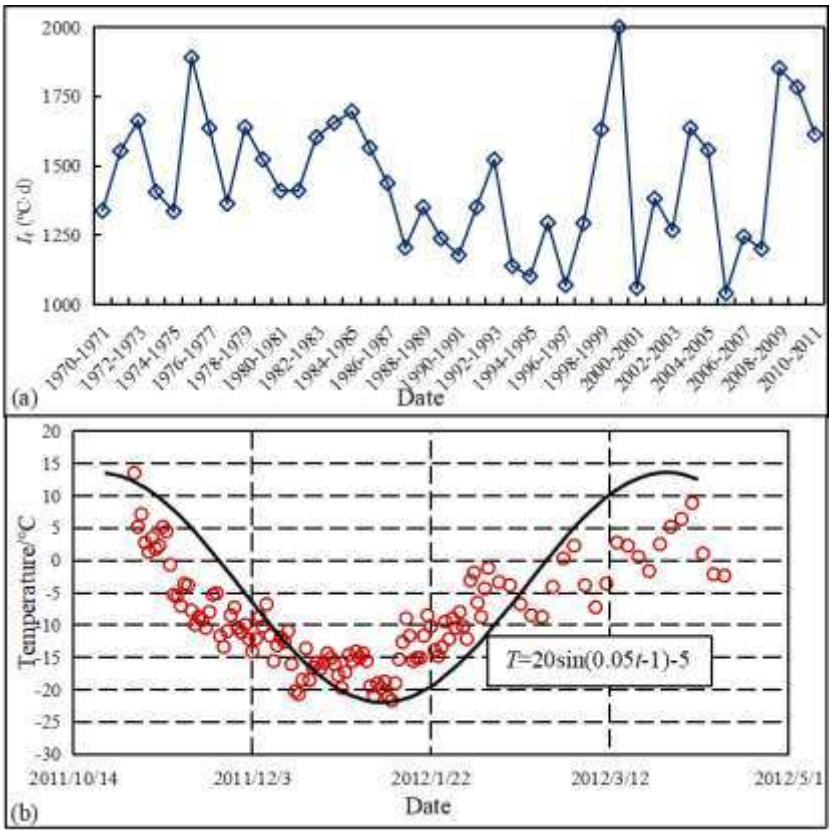

Fig. 3 Temperature characteristics
(a: Freezing index curve, b: Temperature during the freeze-thaw period 2011-2012)

94 The main canal length of the Hada Mountain Water Conservancy Project is 95.93km. The canal
95 cross-section is trapezoidal. Under low temperature conditions, frost damage to the water
96 conveyance canal is a serious problem, which threatens the safety of the project. The polyurethane
97 insulation board + concrete slab slope protection (PC) is designed to reduce the impact of frost
98 damage on the water conveyance canal, and the soil slope is used as comparison tests , the forms of
99 PC and soil slope are shown in Fig. 4.

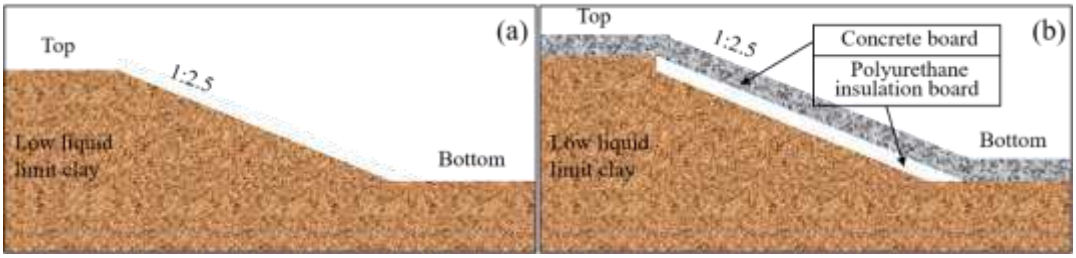

Fig. 4 Diagram of slopes and protection scheme (a: Soil slope, b: PC)

3 Experimental Analysis

3.1 Monitoring methods

To determine the characteristics of freezing depth and groundwater level changes on the slopes of the canal, 25 m test sections are established at three sites (hereafter referred to as 2 km test site, 4 km test site and 47 km test site) in the main canal of the Hada Mountain Water Conservancy Project, and freezing depth and groundwater level monitoring devices are installed as shown in Fig. 5. The freezing depth monitoring devices are buried at a depth of 2.10m. The 47km test site is shown in Fig. 5b and the other two test sites are of the same form.

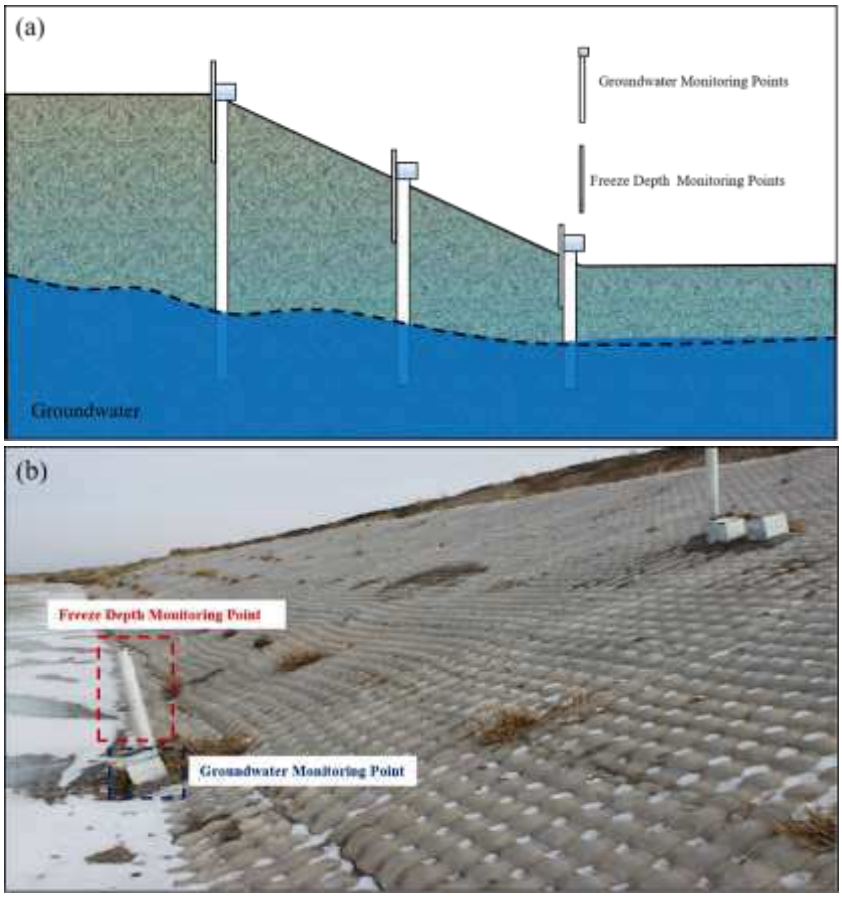

Fig. 5 Freeze depth and groundwater table monitoring points in the test site
(a: Diagram of monitoring points, b: Freeze depth and groundwater table monitoring in the 47km test site)

3.2 Freezing depth and groundwater changes

The changes in groundwater level in the region and the freeze-thaw lines on the soil slopes between 2011 and 2012 are shown in Fig. 6. During the freeze-thaw cycle in the 2011-2012 period, the freezing and thawing curves of the soil and the groundwater curves of the three test sites are similar, with the soil starting to freeze at the beginning of November and the freezing depth of the slopes increasing. By mid-February of the following year, the freeze depth no longer increases. The freeze depth in the 2km and 4km test sites is similar, with a maximum freeze depth of about 200cm at the top of the slope, a maximum freeze depth of about 150cm in the middle and a maximum freeze depth of about 120cm at the bottom. The freeze depth of the soil in the 47km test site is less than the previous two test sites, with a maximum freeze depth of about 160cm at the top of the slope, 140cm in the middle and 120cm at the bottom. The freezing remains until mid-March, when the soil thaws from the surface to the maximum freeze depth. By mid-May, the freezing has almost disappeared. The groundwater level declines as the freeze depth increases. Once the freeze depth becomes stable, the groundwater level remains stable as well. At the beginning of April, the temperature rises and the groundwater level rises rapidly due to the release of water from the canal and the thawing of the soil.

For the same locations, the difference caused by the effects of temperature, wind speed, wind direction and external loads on the freeze depth of soil is small. The main factor contributing to the difference is the effect of the water content of soil. The soil at the bottom of slope has a higher water content than the soil at the top. Because of the effect of the latent heat of phase change in water and ice, the temperature at the bottom of the slope is relatively higher than that at the top, therefore the

freeze depth at the bottom is shallower than that of the top. When 5 and 6 cm polyurethane insulation boards + concrete boards are used for slope protection, the freeze depth is measured at the top of the slope. As shown in Fig. 7, as the insulation boards become thicker, the freeze depth of the soil becomes shallower. Compared to the freezing depth in soil slopes, the slope protection structure proposed in this paper can significantly reduce the freeze depth which is about 80-100cm. Besides that, the slope thawing is advanced under this type of slope protection, and the freeze of water disappears in mid-April, with the freeze of water disappearing almost a month earlier.

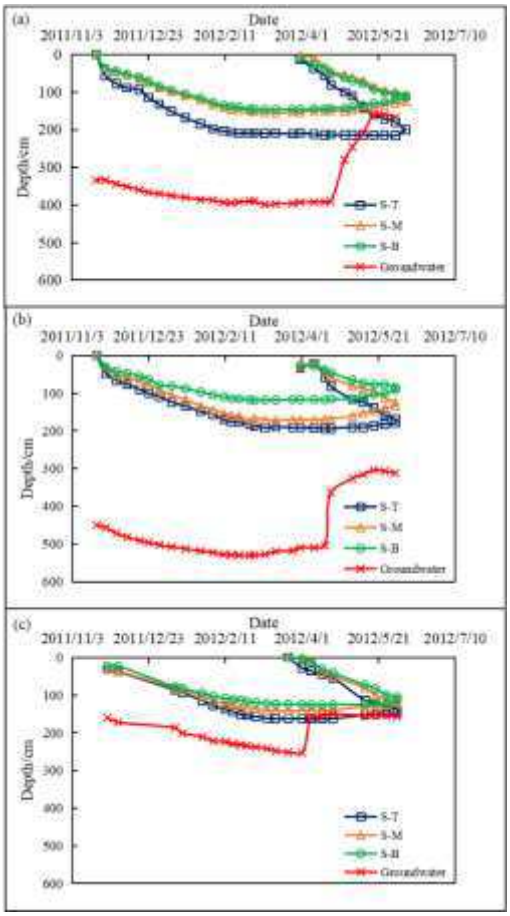

Fig. 6 Soil slope - Groundwater, freeze depth monitoring curve (a: 2km test site, b: 4km test site, c: 47km test site. S: Slopes, T-top of slope, M-middle of slope, B-bottom of slope.)

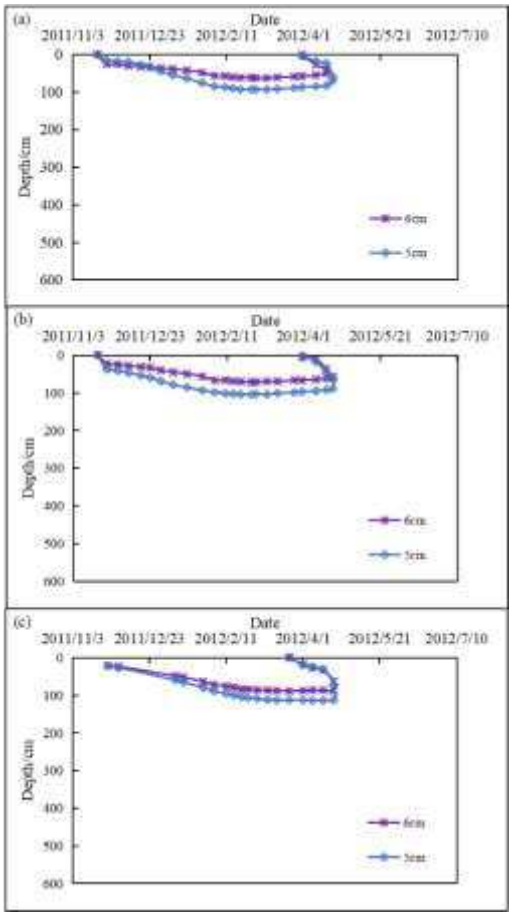

Fig. 7 PB - Groundwater, freeze depth monitoring curve (a: 2km test site, b: 4km test site, c: 47km test site)

3.3 Water content changes in the soil before and after freezing

In section 3.2, the effect of water content on the freeze depth of soil is discussed. To further verify the conclusions, the water content of soil is measured before and after freezing at different

depths of the top, middle and bottom of slope, taking the soil slope of the 47km test site as an example. The soil water content - depth variation curve is shown in Fig. 8. As shown in the figure, before freezing, the water content of surface soil in all three locations of slope is around 10%, in the range of 0-60cm below the surface, the water content increases with depth. The high water content of topsoil may be related to the infiltration of surface water. The bottom of slope is close to the water in canal and the water content of soil at bottom is relatively higher than the other two locations due to the action of the flowing water. After the water in soil freezes, the water content of topsoil decreases slightly, associated with the sublimation of ice. In deeper depth, as the ice front progresses downwards, unfrozen water gradually migrates towards the ice front, thus causing the water content of soil to be greater than that before freezing. Due to the migration of water in soil, under the maximum freeze depth, the water content of soil after freezing is lower than that before freezing. Among the three test sites, the water content of soil at the bottom of slope is the highest and the latent heat of phase change is higher, thus the freeze depth at the bottom of slope is less than that at the other two locations on the slope.

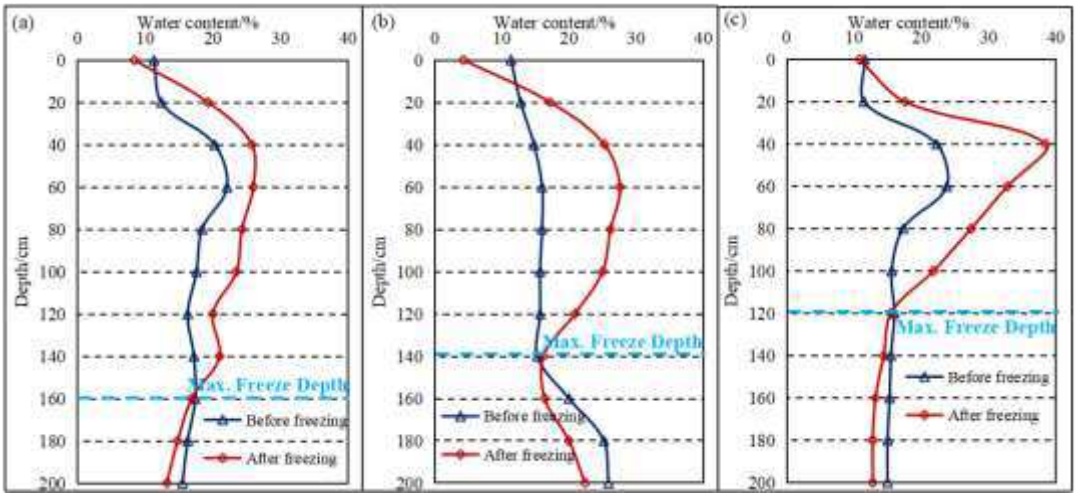

Fig. 8 Moisture content change curve of the soil before and after freezing
(a: Top, b: Middle, c: Bottom)

4 Numerical model for hydrothermal coupling incorporating phase change effects

Seasonal freeze regions are affected by temperature and water freeze ins soil causing frost damage. Philip and De Veries (1957)[21] first proposed the theory of hydrothermal coupling and proposed a nonlinear hydrothermal coupling model based on the principle of viscous fluid flow and heat balance in porous media. Under this basis, several numerical models of hydrothermal coupling have been proposed, and the problem of hydrothermal coupling of geotechnical engineering in cold regions has been successfully solved. The study of hydrothermal coupling has been gradually developed. The application of hydrothermal coupling has been increasing recently, and the following assumptions are made in the hydrothermal coupling model to improve the efficiency of the calculation[22]:

1) The soil medium is a homogeneous isotropic pore medium consisting of unfrozen water, ice and soil skeleton, which does not deform during the freeze process.

2) Water migration in the geotechnical medium, without the contribution of air to water migration.

3) The latent heat and heat transfer processes of water ice phase change are calculated.

Under the assumptions above, modelling is carried out by temperature and water fields and the different physical field control conditions are as follows.

4.1 Water field equations

The migration of unfrozen water in the soil follows Darcy's law[23]. Using the Storage Model node, the Darcy's Law interface contains an implementation of Darcy's law which explicitly

includes an option to define the linearized storage S (1/Pa) using the compressibility of the fluid and the porous matrix[24]:

$$Q_m=\rho_s S\frac{\partial p}{\partial t}+\nabla\cdot\rho[-\frac{\kappa}{\mu}(\nabla p+\rho g\nabla D)] \quad (3)$$

Where: Q_m is the mass source, which expresses as ice melting water, calculated according to Eq. 4; ρ is the density of the soil (kg/m³); t is time (s); S is the water transfer model calculated according to Eq. 5; p is the pressure (kPa); g is the acceleration of gravity (m/s²); μ is the dynamic viscosity (Pa·s); κ is the hydraulic conductivity (m/s); D the diffusivity of water in frozen soil.

$$Q_m=S_w\cdot e(\rho_i-\rho_w)\frac{\partial S_w}{\partial t} \quad (4)$$

Where: S_w is the saturation of unfrozen water in the soil; e is the porosity ratio of the soil, as the water in the soil freezes, the pores are blocked by ice, resulting in a lower porosity ratio, which can be calculated according to Eq. 6; ρ_i, ρ_w are the densities of ice and water respectively (kg/m³).

$$S=S_w\cdot e\cdot\beta \quad (5)$$

Where: β is the effective compression factor, which is a combined value of water, ice, and solid matrix compressibility. When considering the ice-water phase change, the saturation of unfrozen water in the soil, S_w, depends on the phase change and can be calculated as in Eq. 7.

$$e=e_0\cdot S_w \quad (6)$$

Where: e_0 is the initial porosity ratio.

$$S_w=S_r+(1-S_r)\cdot\theta_2 \quad (7)$$

$$\theta_1+\theta_2=1 \quad (8)$$

Where: S_r is the residual liquid water saturation, θ_1, θ_2 is a smooth step function defined in the Phase Change Material node. The step function θ_2(T) is zero for temperatures below the melting temperature T_{pc}, and it equals 1 for temperatures above T_{pc}. In the INTERFROST benchmark, it is

assumed that the mushy ice zone extends from 0°C to -1°C. Therefore, T_{pc} is set to -0.5°C and the transition interval of θ_2 is defined as 1K to represent this.

Considering the ice-water phase change, the ice clogs the porosity in the soil, leading to a reduction in the porosity ratio, and this leads to a lower permeability of the soil. k expressed in terms of saturation S_w can be calculated by Eq. 9.

$$k=k_s \cdot 10^{-I \cdot e \cdot (1-S_w)} \tag{9}$$

Where: k_s is the coefficient of permeability of saturated soil (m/s); I is the impedance factor.

4.2 Temperature field equations

The differential equation for heat conduction in frozen soil is:[25].

$$(\rho_s C)_{eq} \frac{\partial T}{\partial t} + \rho_s C_w \boldsymbol{u} \cdot \nabla T + \nabla \cdot (-k_{eq} \nabla T) = Q \tag{10}$$

Where: T is the temperature of the soil at different moments (°C); C is the heat capacity at constant pressure (J/(kg·°C)).

4.3 Model validation

To simplify the calculations, a numerical model is constructed based on the 47km test section among the three test sites of this paper. The numerical simulation calculation model and the dimensions of each part are shown in Fig. 9. The model contains 5544 grid vertices and 10521 elements, with boundaries a-e-f-b for the natural ground surface. The temperature boundary of condition shown in Eq. 2 is imposed, with an initial value of 15°C. The specific material parameters as shown in Table 1. In the water field, the soil is considered to be unsaturated. The boundaries are set as zero flux boundaries and the water field calculation parameters are shown in Table 2. The

transient calculation method is used to calculate the freeze depth and the change in water content of the soil over 200 days and the freeze depth and the change in water content are monitored at the three locations marked by the dotted lines.

Table1 Material properties

Material	ρ（kg/m^3）	C(J/kg·℃)	λ(W/m·℃)
Clay	1910	1460	2.50
Water	1000	4200	0.63
Ice	918	2100	2.31

Table 2 Parameters for seepage models of unsaturated soils

Parameters	I	e_0	μ(Pa·s)	w_{sat}	S_w	S_r	k(m/s)
Clay	50	0.3	1.793e-3	0.35	0.68	0.14	9.62×10^{-7}

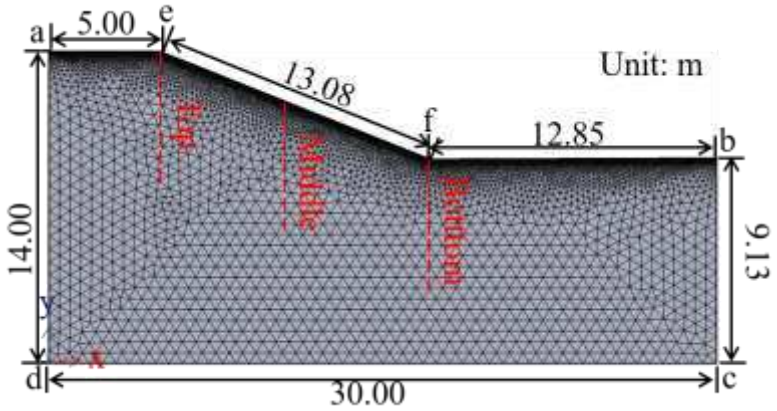

Fig. 9 Numerical calculation model

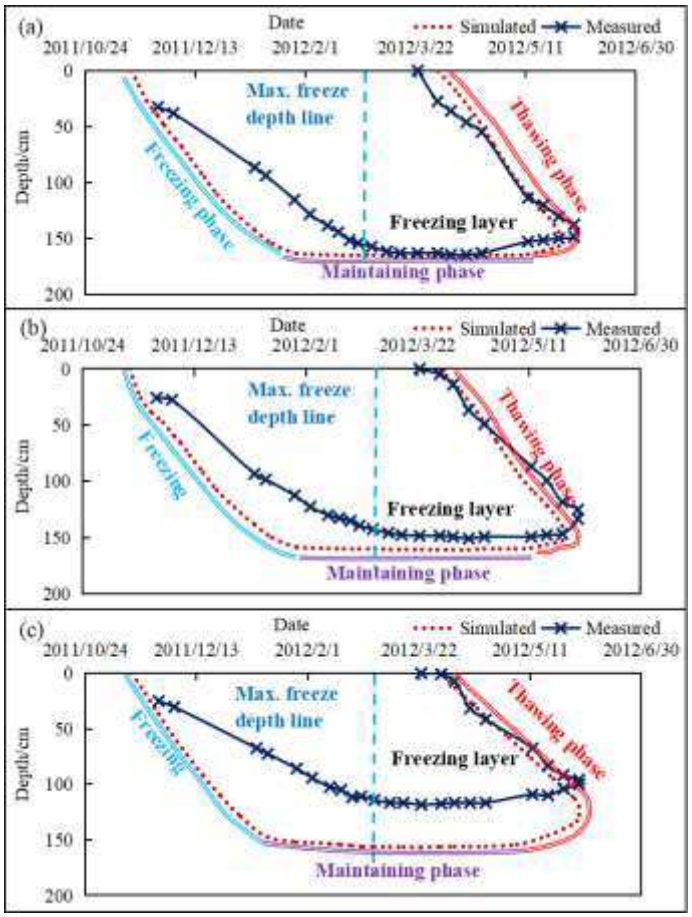

Fig. 10 Freeze-thaw curves for slopes
(a: Top, b: Middle, c: Bottom)

223 The measured and simulated values of freeze-thaw process at the top, middle and bottom of
224 slope in a single freeze-thaw cycle are shown in Fig. 10. Although there is a deviation between the
225 simulated and measured values, with a maximum deviation of about 0.3m. This difference is mainly
226 caused by the fact that the temperature boundary conditions in numerical calculation are fitted to
227 the measured results. The actual temperature boundary conditions in the field are influenced by solar
228 radiation, wind direction and speed as well as rainfall, making it impossible to fully introduce the
229 computational model. However, the results of the simulations still reflect the freeze-thaw process
230 on the slopes. Comparing the results, it is clear that the freeze process manifests three main stages
231 during a freeze-thaw cycle.

232 (1) Freeze developing phase: during this phase, the ice front develops downwards due to the

decrease in temperature leading to an increasing to freeze depth.

(2) Freeze maintenance phase: When the ice front surface develops to a certain depth, the ice front neither retreats nor continues to develop and remains stable.

(3) Thawing phase: In this phase, the temperature warms up to greater than 0°C and the frozen soil begins to thaw until the soil is no longer frozen.

The distribution characteristics and change processes between measured and simulated freezing/thawing depths are similar. The numerical results show that the numerical model developed in this paper for calculating the slope of water conveyance channel is reliable and can be applied to the analyses of the temperature-freeze depth-water content.

4.4 Temperature - freeze depth - water content regime

The main factor influencing water migration is the coupling of the temperature and water fields during soil freezing and thawing, i.e. the movement of water under the effect of temperature gradients[28]. The temperature distribution of the numerical simulation is shown in Figs. 11 and 12, with the initial temperature field set at 15°C in mid-October. The water in soil freezing occurs at the end of November 2011, and the freeze depth gradually increases as the temperature decreases. Water freeze reaches the maximum freeze depth at the end of February 2011 and remains stable. Comparing the temperature variation curves at different depth for the three locations, the freeze depth at the top and middle of slope is around 160cm, and the freeze depth at bottom is around 150cm. As the temperature decreases, the water in the pores gradually freezes and the water content decreases.

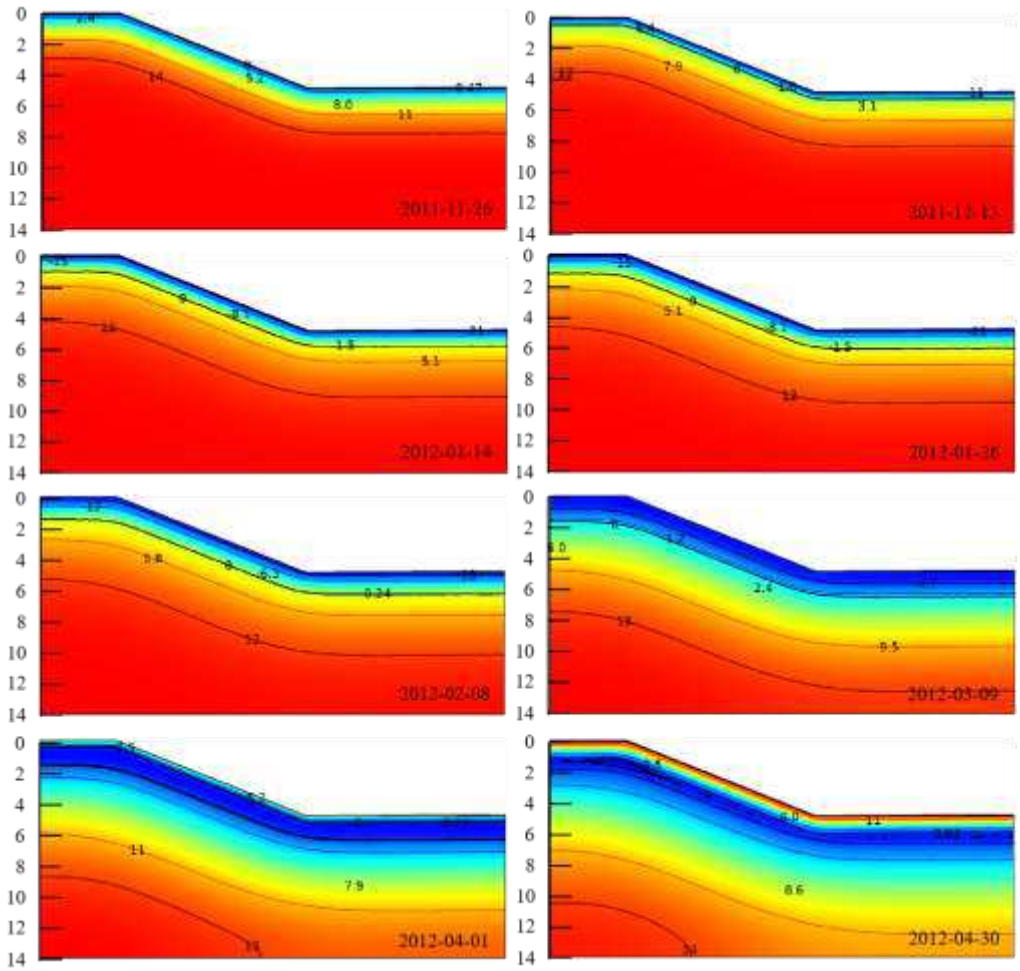

Fig. 11 Temperature field distribution at different times(unit: ℃)

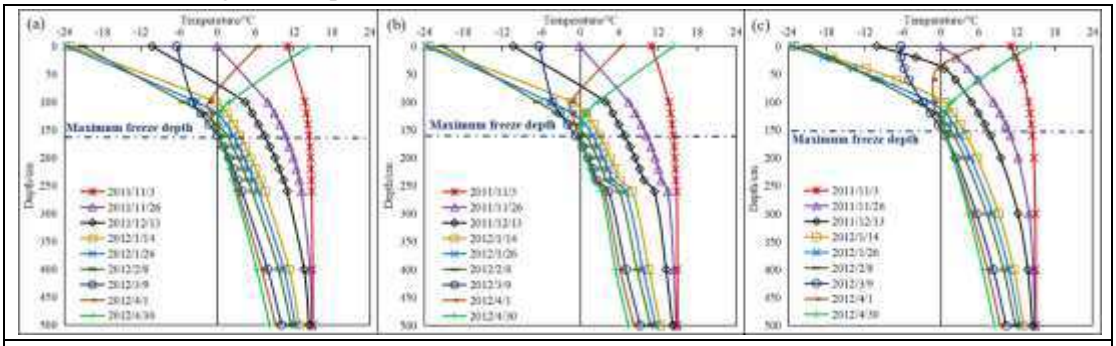

Fig. 12 Temperature variation curves
(a: Top, b: Middle, c: Bottom)

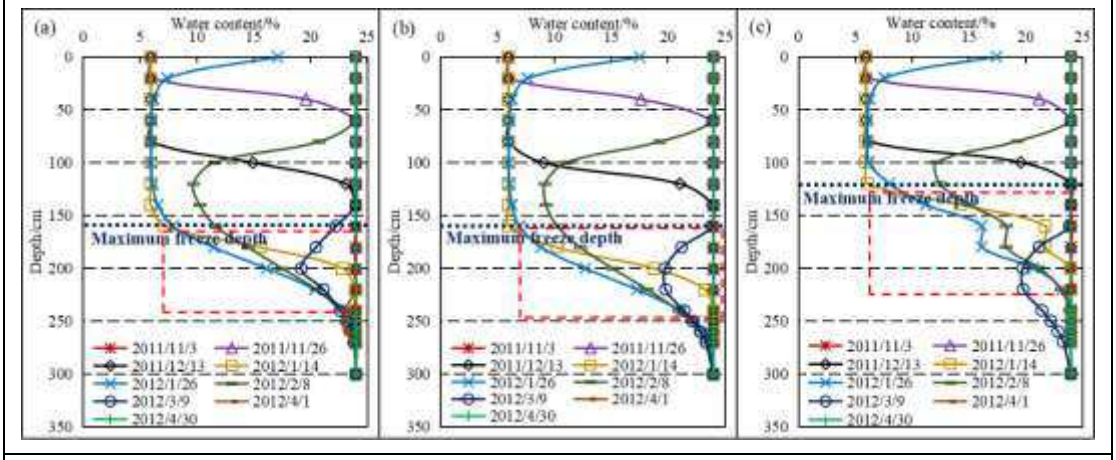

Fig. 13 Water content variation curves
(a: Top, b: Middle, c: Bottom)

The change in water content during the conversion of water to ice is shown in Fig. 13. As shown in the figure, the water content is 0.24 at the beginning of November. In late November, the water in soil freezes to a depth of around 50cm. At this time, the soil below 50cm has not frozen and the water content remains at the initial water content. After the freeze depth remains stable in mid-February the following year, the water content remains stable at the same time. When the temperature warms up in late March, the ice in the soil about 150cm below the surface gradually thaws and melts, and the water content returns to its initial value. The curves of water content show that after the water freezes, the water content of soil below the maximum freeze depth also decreases. It is not until the freeze has completely melted that the water content gradually returns to its initial value, which is inextricably related to the water migration during the freezing process.

4.5 Anti-frost structures on the slopes of water conveyance canals

Water conveyance canal projects in seasonal freeze regions are often damaged by the freeze-thaw action of the soil. Therefore, anti-frost structures should be adopted to eliminate or reduce the soil freeze, which can effectively reduce the risk of damage to the slope. According to the measured and simulated values in the previous sections, the degree of freeze is mainly influenced by

268 temperature as well as water content. Therefore, the insulation boards are most commonly used for
269 insulated, water-insulated. According to the results of anti-frost heave tests on insulation boards in
270 the test areas, the small thermal conductivity of polyurethane material enables the heat balance
271 between heat absorption and heat release, thus resulting in the subsoil not being frozen. For further
272 determination of insulation board thickness, a structural form (concrete board + insulation board)
273 as shown in Fig. 14 is used for anti-frost simulation.

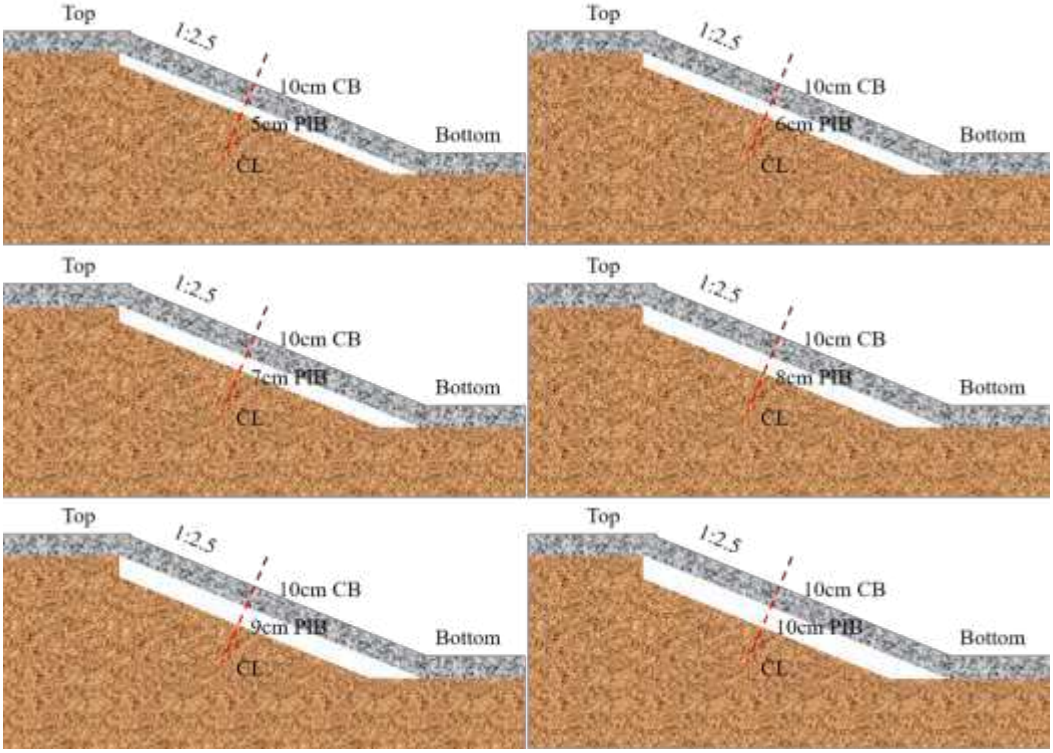

Fig. 14 Anti-frost structures on the slopes of water conveyance canals in seasonal frozen regions

274 Based on the numerical model established in this paper, the maximum freeze depth distribution
275 can be computed. For the convenience of modelling, a thin layer boundary condition is used instead
276 of the insulation board solid mesh. The insulation board, as well as concrete material parameters,
277 are shown in Table 3.

278 Table 3 Parameters of Insolation boards and Concrete Boards

Material	λ(W/m·°C)	ρ（kg/m^3）	C(J/kg·°C)
Concrete	1.800	2500	880.0
PIB	0.026	48	1330.0

The results of the temperature field simulations are shown in Fig. 15, where the 0°C isotherms are used as the maximum freeze depth. The changes in freeze depth and water content at the three locations are shown in Table 4.

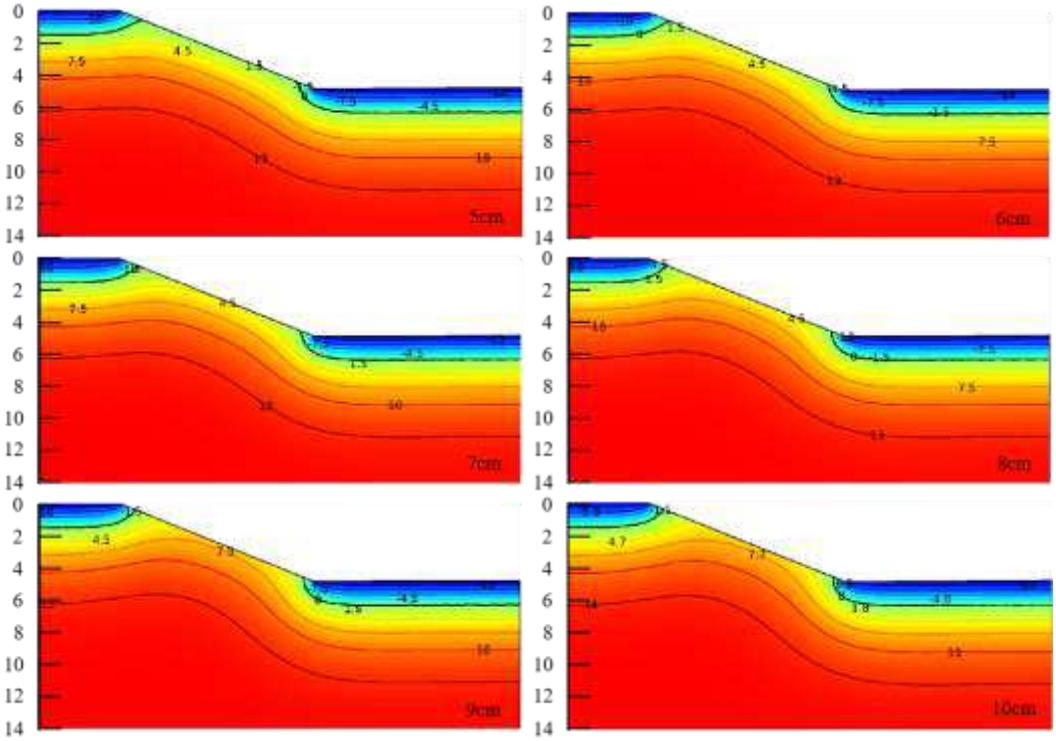

Fig. 15 Temperature fields of the six anti-frost structures at maximum frost depth time

Table 4 The Max. Frost Depth and Water Content for the six anti-frost structures.

PIB	T		M		B	
	Freeze Depth/cm	Water Content/%	Freeze Depth/cm	Water Content/%	Freeze Depth/cm	Water Content/%
0	165	6.0	160	5.9	156	9.7
5	120	14.3	0	24.0	100	14.8
6	119	14.8	0	24.0	98	14.8
7	117	14.9	0	24.0	96	14.9
8	115	14.8	0	24.0	95	14.7
9	113	14.6	0	24.0	94	14.7
10	112	15.1	0	24.0	93	14.9

Comparing the effect of different thicknesses insulation board on anti-frost, it shows that 5 and 6 cm insulation boards can significantly reduce the freeze depth. The effect of increasing the thickness of the insulation boards on reducing the freeze depth does not change significantly. In actual engineering applications, increasing the thickness of the insulation boards is undoubtedly

increasing the cost of project, but the effect of improving the insulation boards is not obvious. According to the research of this paper, the insulation board thickness of 5-6cm can improve the anti-frost capacity of the slope. Regions with serious frost damage can refer to the research results of this paper and increase the thickness of the insulation boards appropriately. Comparing the water content at maximum freeze depth, it shows that at the maximum freeze depth of the unprotected slope, the water content of the soil remains at the residual water content, i.e. almost all of the water in the soil is frozen. However, although the water content of soil with protective structures decreases, the unfrozen water content of the soil remains at around 14.8%. With the protection of the insulation boards, the freezing action reduces and the water at the maximum freeze depth cannot freeze sufficiently.

In the middle of the slope, under the protection of polyurethane insulation boards, the freeze depth is almost negligible and differs considerably from the actual situation. This is because of simplification of the boundary conditions in numerical calculations and the fact that external factors (solar radiation, wind speed, wind direction and precipitation, etc.) are not considered in the calculation process. Therefore, the results obtained differ considerably from reality, but they still illustrate the usability of polyurethane boards in the design of anti-frost structures. Comparing the freeze depth at the top to bottom of slopes, it shows that the error between the simulated and measured values is around 10-20cm, which is a desirable result and can be used as a reference for design of water conveyance canals to prevent freezing.

5 Discussion

5.1 Characteristics of temperature and freeze depth change in seasonal freeze regions

In seasonal freeze regions, the water in soil freezes under the clod temperature[29]. The temperature changes dramatically from the ground surface to the maximum freeze depth—a process that directly affects the direction and intensity of water migration[28]. In this paper, the trend of soil freeze depth is summarized in Fig. 16 by field tests as well as numerical simulations. As shown in the figure, the temperature gradually drops from late October to early November each year, causing the water in soil to freeze. Thereafter, the freeze depth has increased until the February of the following year, when it reaches the maximum freeze depth. After the maximum freeze depth remains until March, the temperature increases to above zero and the soil melts in both directions from the surface and the maximum freeze depth, at the end of April the freezing of the soil generally disappears.

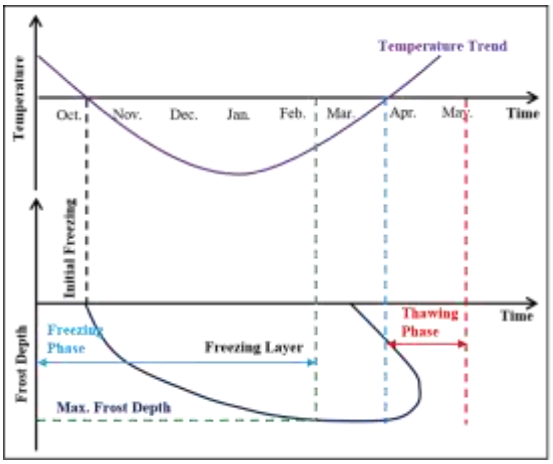

Fig. 16 Frost Depth-Time Curve

5.2 Characteristics of temperature and water variation in seasonal freeze regions

The temperature at the surface in seasonal freeze regions varies widely depending on the seasons, resulting in differences in temperature from the surface to the maximum freeze depth[28,30]. For example, at different locations on the slopes, the freeze depth varies between

shaded and sunny slopes[31,32].

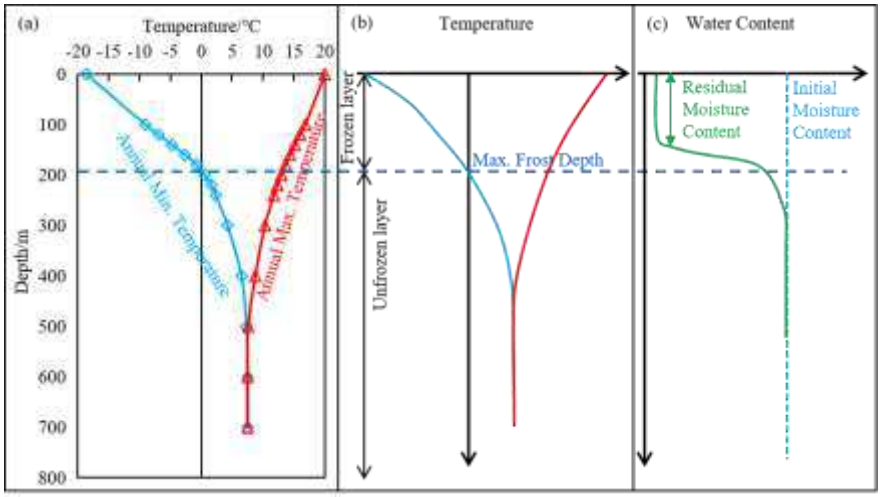

Fig. 17 Characteristics of Temperature-Depth- Water content variation in the seasonal frozen regions (a: Simulated Value, b: Tempeture-Depth Trend, c: Water Content-Depth Trend)

The freeze depth also varies as shown in Fig. 17. As the temperature decreases, the water in soil gradually freezes from the surface downwards the maximum freeze depth (Fig. 17a), this part of the soil layer is called the Frozen Layer and below the Frozen Layer is the Unfrozen Layer. The freeze depth affects the water content of soil (Fig. 17c). In the simulations of this paper, the water storage model in Comsol software is applied to fully investigate the effect of freeze water on the soil porosity ratio as well as the permeability coefficient, and the results are more reflective of the hydrothermal coupling during the freezing and thawing process. The water content of soil in the frozen layer decreases to the residual water content. Although freezing does not occur below the maximum freeze depth, the water content of the soil under the maximum freeze depth also decreases. This is because the ice front is constantly developing downwards during the freezing process, and water migration occurs under the influence of temperature as well as soil pore capillary forces, resulting in a decrease in the water content of the soil below the maximum freeze depth. After the soil has completely melted, water migration occurs by gravity and the water content of the soil gradually converges to its original state.

6 Conclusions

This paper investigates the characteristics of temperature - freeze depth - water content of the slope based on the combination of field tests and numerical simulations, and compares the effect of different thicknesses of polyurethane materials, and the following conclusions are drawn.

1) As the temperature decreases, the ice front gradually develops downwards, making the water migration path decrease, which is beneficial to water migration. After the water freezes to the maximum freeze depth, the water content of soil below the maximum freeze depth is less than the initial water content, which is inseparably related to water migration.

2) When polyurethane material is used for anti-frost protection, the freeze depth of soil decreases significantly, which is beneficial for the safety of the canals. The results of the insulation board tests in the field as well as the numerical simulations show that the thicker the insulation board, the smaller the freeze depth of the soil. However, in actual construction, increasing the thickness of insulation boards is undoubtedly an increase in the cost of the project, thus using the proper thickness of insulation boards for protection can save costs. The research in this paper shows that 6-7cm polyurethane insulation boards can effectively decrease freeze depth and thus protect the slope.

The thickness and temperature distribution of the frozen layer in seasonal frozen soil areas are important factors influencing the damage of water conveyance canals. Increasing the heat entering slope or reducing the heat diffusion of soil is an effective method to reduce the freezing, and the polyurethane insulation boards can precisely meet such requirement. Therefore, such materials have good prospects for application in the prevention of freezing.

Acknowledgements

This work was supported by the National Natural Science Foundation of China (Grant Nos. 41972267

Reference

[1] Mo Tengfei, Lou Zongke.(2020). Numerical Simulation of Frost Heave of Concrete Lining Trapezoidal Channel Under an Open System. *Water*(2). DOI:10.3390/w12020335.

[2]Zhou Youwu, Guo Dongxin, Qu Guoqing.(2000). Geocryological regionalization and classification map of the frozen soil in China (1:10,000,000). A Big Earth Data Platform for Three Poles, 2011. DOI: 10.11888/Geocry.tpdc.270037. CSTR: 18046.11.Geocry.tpdc.270037.

[3]Wang Zhengzhong, Jiang Haoyuan, Wang Yi, Liu Quanhong, Ge Jianrui.(2020). Research progresses and frontiers in anti-seepage and anti-frost heave of canals in cold-arid regions. *Transactions of the Chinese Society of Agricultural Engineering.* (22),120-132. DOI:CNKI:SUN:NYGU.0.2020-22-014.

[4]Ge Shudong.(2004). Research on Structure of Anti-seepage Channels in Seasonal Frozen Soil Region. Master Degree thesis, Hohai University, Nanjing (in Chinese).

[5]Chen Tao.(2004). Establishment and Application of Mechanics Model of Frost Heaving Damage of Concrete Lining Open Canal. Master Degree thesis, Northwest A&F University, Xi'an (in Chinese).

[6]Li JL (2009) Mechanics models of frost-heaving and the research of anti-frost heave structure for lining canal. Ph.D. Dissertation for Northwest A&F University, Yangling (in Chinese).

382 [7]Ye Zhihui, Wu Jiandong.(2020). Analysis of development in study of irrigation canal seepage
383 control techniques in farm fields in China. *Water Resources Planning and Design*,
384 (06):113-115+167.
385 [8]Taber Stephon.(1930). The Mechanics of Frost Heaving. *Journal of Geology*, 38(4): 303-317.
386 DOI:10.1086/623720.
387 [9]Everett D H.(1961). The thermodynamics of frost damage to porous solids. *Transactions of the*
388 *Faraday Society*, 57: 1541-1551. DOI:10.1039/tf9615701541.
389 [10]Jackson K A.(1966). Frost heave in soils. *Journal of Applied Physics*, 37(2): 848.
390 DOI:10.1063/1.1708270.
391 [11]Miller R D.(1972). Freezing and heaving of saturated and unsaturated soils. *Highway Research*
392 *Record*, 393: 1-11. DOI: 10.1021/ba-1972-0110.ap001.
393 [12]Lundin Lars-Christer.(1990). Hydraulic properties in an operational model of frozen soil.
394 *Journal of Hydrology*, 118(1-4), 289-310. DOI:10.1016/0022-1694(90)90264-X.
395 [13]Hu Da, Yu Wenbing, Lu Yan, Chen Lin, Liu Weibo(2019). Experimental study on unfrozen
396 water and soil matric suction of the aeolian sand sampled from Tibet Plateau. *Cold*
397 *Regions Science and Technology*, 164102784-102784.
398 DOI:10.1016/j.coldregions.2019.102784.
399 [14]Kunio Watanabe, Yurie Osada.(2016). Comparison of Hydraulic Conductivity in Frozen
400 Saturated and Unfrozen Unsaturated Soils. *Vadose Zone Journal*, 15(5), 1-7.
401 DOI:10.2136/vzj2015.11.0154.
402 [15]Li Zhuo, Liu Sihong, Feng Youting, Zhang Chenchen.(2013). Numerical study on the effect of
403 frost heave prevention with different canal lining structures in seasonally frozen ground

regions. *Cold Regions Science and Technology* 85,242-249.DOI:10.1016/j.coldregions.2012.09.011

[16]Li Shuangyang, Lai Yuanming, Pei Wansheng, Zhang Shujuan, Zhong Hua. (2014). Moisture-temperature changes of freeze-thaw hazards on a canal in seasonally frozen regions. *Nat Hazards*, 72(2): 287-308. DOI:10.1007/s11069-013-1021-3.

[17]Li Shuangyang, Zhang Mingyi, Tian Yibin, Zhong Hua.(2015). Experimental and numerical investigations on frost damage mechanism of a canal in cold regions. Cold Regions Science and Technology, 1161-11. DOI:10.1016/j.coldregions.2015.03.013.

[18]Li Shuangyang, Lai Yuanming, Zhang Mingyi, Pei Wansheng, Yu Fan.(2019). Centrifuge and numerical modeling of the frost heave mechanism of a cold-region canal. Acta Geotechnica, 14(4), 1113-1128. DOI:10.1007/s11440-018-0710-1

[19]Li Jingjun, Zhou Bolin.(2019). Simulation for Frost Heaving Damage of Concrete Lining Channels by Using XFEM. *Journal of Coastal Research*,93(sp1), 264-273.DOI:10.2112/SI93-035.1

[20]Li Zhuo, Liu Sihong, Zhang Chenchen. (2013). Experimental study on the effect of frost heave prevention using soilbags. *Cold Regions Science and Technology*,(85),109-116. DOI:10.1016/j.coldregions.2012.08.008.

[21]Philip J R, De Veries D A.(1957). Moisture movement in porous material under temperature gradient. *EOS: Earth & Space Science News*,(2),222-232.DOI:10.1029/TR038i002p00222.

[22]Tan Xianjun, Chen Weizhong, Tian Hongming, Cao Junjie.(2011).Water flow and heat transport including ice/water phase change in porous media: Numerical simulation and application.

426 *Cold Regions Science and Technology*,(1-2). DOI:10.1016/j.coldregions.2011.04.004.

427 [23]Bai Qingbo, Li Xu, Tian Yagao，Fang Jianhong. (2015). Equations and numerical simulation

428 for coupled water and heat transfer in frozen soil. *Chinese Journal of Geotechnical*

429 *Engineering*,(S2), 131-136. DOI:CNKI:SUN:YTGC.0.2015-S2-027.

430 [24]https://cn.comsol.com/models

431 [25]Luo Qing.(2019). Heat transfer, Second edition. Chongqing University Press, Chongqing,China.

432 [26]Lu Ning(U.S.), William J. Likos.(2012) Unsaturated soil mechanics. Higher Education

433 Press,Beijing, China.

434 [27]Xu Xuezu, Deng Yousheng.(1991). Experimental study of water migration in permafrost,

435 First edition. Science Press, Beijing, China.

436 [28]Tai Bowen,Yue Zurun,Sun Tiecheng,Qi Shouchen,Li Lei & Yang Zhihao.(2021).Novel anti-

437 frost subgrade bed structures a high speed railways in deep seasonally frozen ground

438 regions: Experimental and numerical studies. *Construction and Building Materials*(269),.

439 DOI:10.1016/J.CONBUILDMAT.2020.121266.

440 [29]Wu X.Y., Niu F.J., Lin Z.J., Shao Z.J. (2017).Delamination frost heave in embankment of high

441 speed railway in high altitude and seasonal frozen region. Cold Regions Science and

442 Technology(153),25-32. DOI:10.1016/j.coldregions.2018.04.017.

443 [30]Zhang Chaochao,Li Dongwei,Chen Junhao,Chen Guanren,Yuan Chang,Wang Zecheng, Zhao

444 Xiao Dong.(2021).Research on the Temperature Field and Frost Heaving Law of Massive

445 Freezing Engineering in Coastal Strata. *Advances in Materials Science and*

446 *Engineering*(2021). DOI:10.1155/2021/5575940.

447 [31]Hua Liu, Fujun Niu, Yonghong Niu, Jing Luo.(2012).Experimental and numerical investigation

448 on temperature characteristics of high-speed railway's embankment in seasonal frozen
449 regions. *Cold Regions Science and Technology*(81),55-64.
450 DOI:10.1016/j.coldregions.2012.04.004.
451 [32]Yu-Zhi Zhang, Yan-Liang Du, Bao-Chen Sun.(2015).Temperature distribution analysis of high-
452 speed railway roadbed in seasonally frozen regions based on empirical model. *Cold*
453 *Regions Science and Technology*(114),61-72. DOI:10.1016/j.coldregions.2015.02.010.

Figures

Figure 1

Frost damage to canals

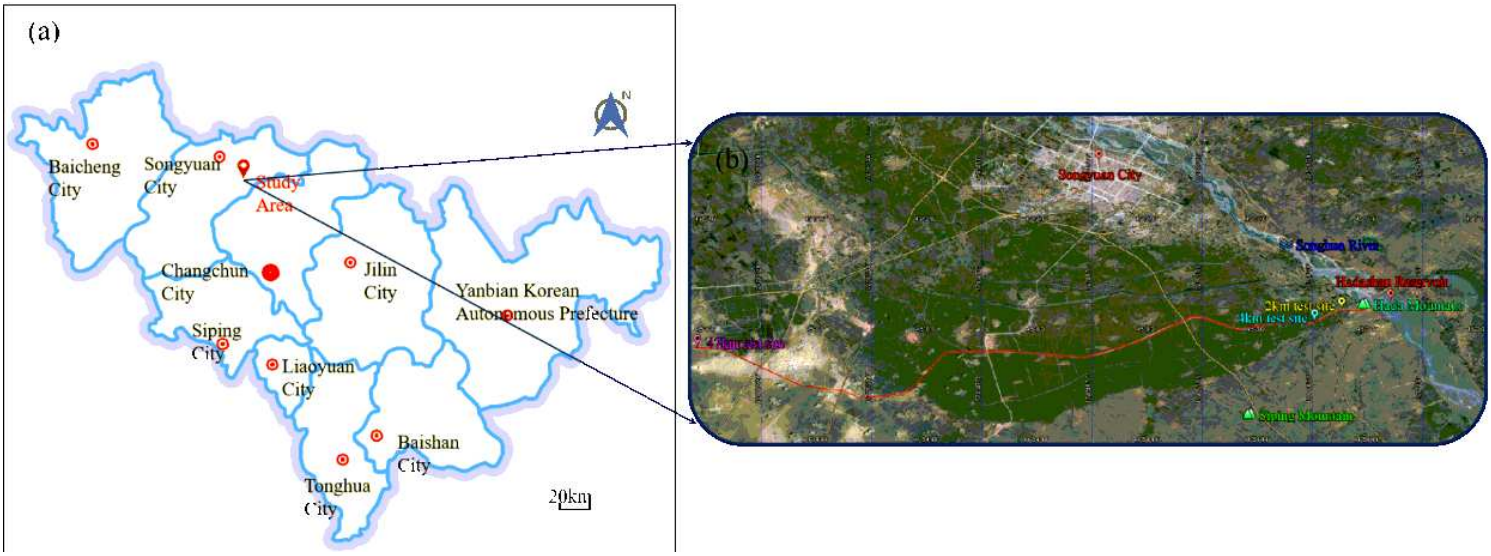

Figure 2

Detailed overview of main canal of Hada Mountain Water Conservancy Project (a: Geographical location map of the study area; b: Satellite map of the study area, c: Soil slope, d: Insulation board and Concrete board slope protection) Note: The designations employed and the presentation of the material on this map do not imply the expression of any opinion whatsoever on the part of Research Square concerning the legal status of any country, territory, city or area or of its authorities, or concerning the delimitation of its frontiers or boundaries. This map has been provided by the authors.

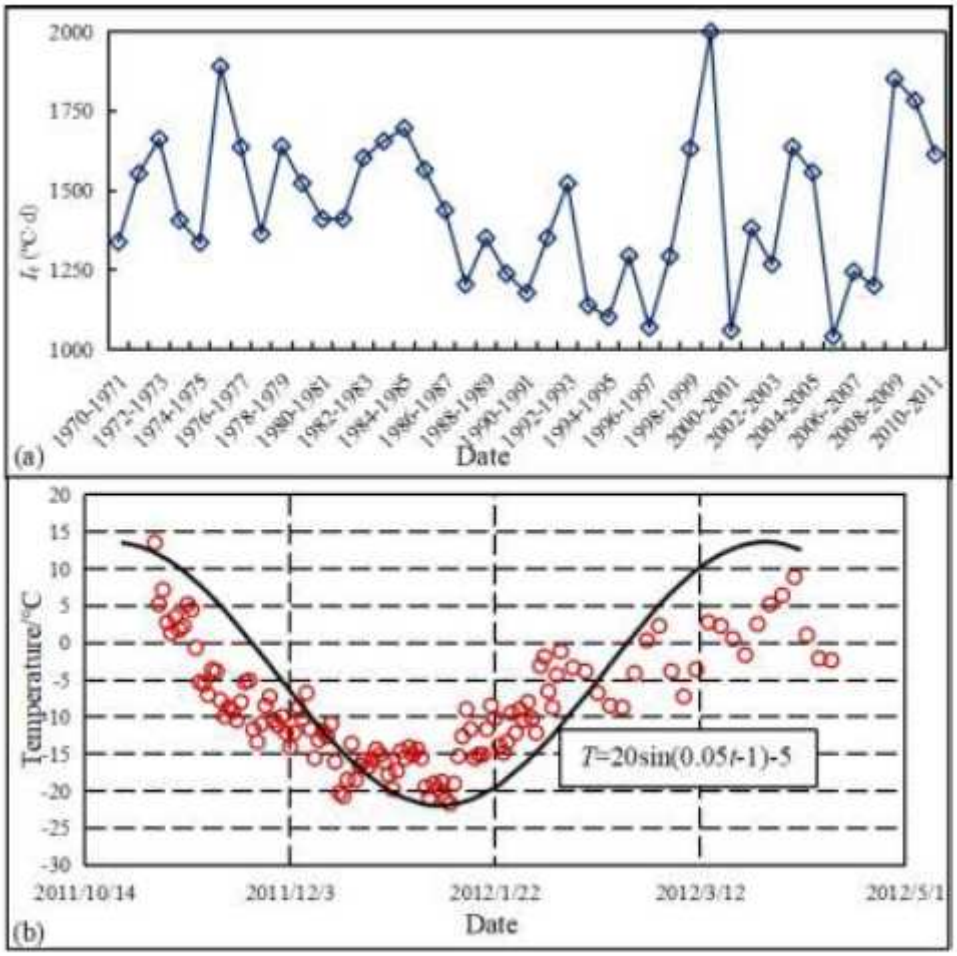

Figure 3

Temperature characteristics

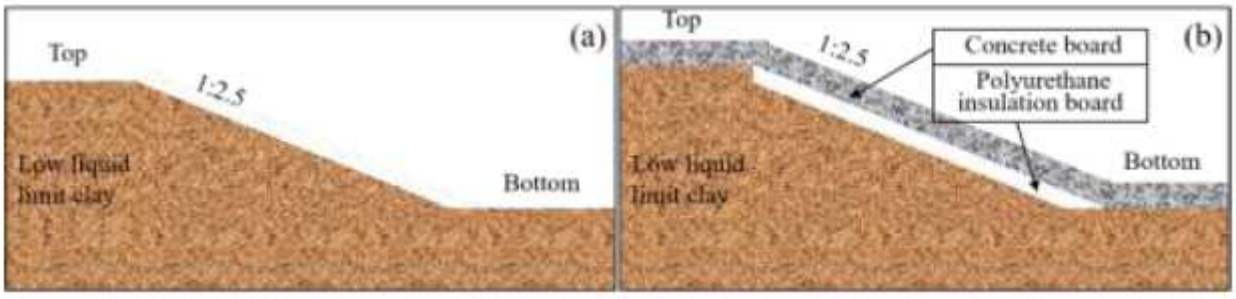

Figure 4

Diagram of slopes and protection scheme (a: Soil slope, b: PC)

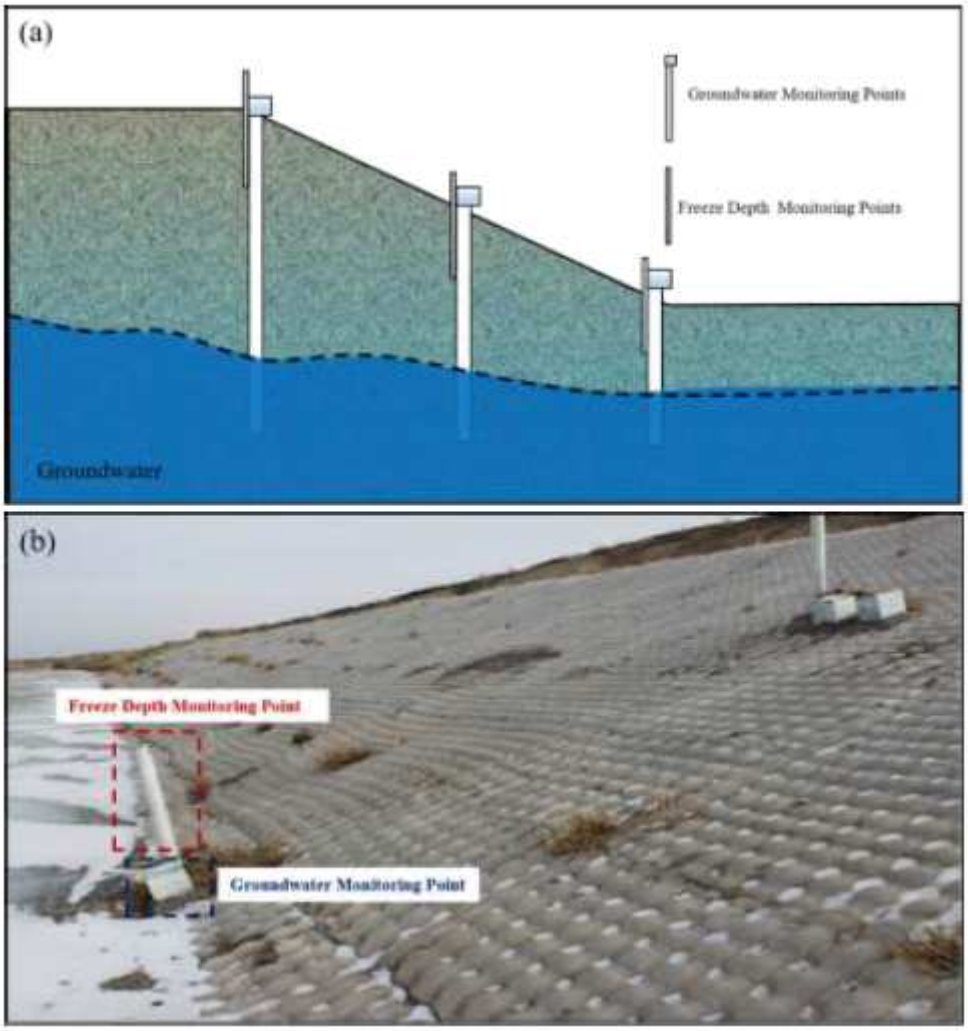

Figure 5

Freeze depth and groundwater table monitoring points in the test site (a: Diagram of monitoring points, b: Freeze depth and groundwater table monitoring in the 47km test site)

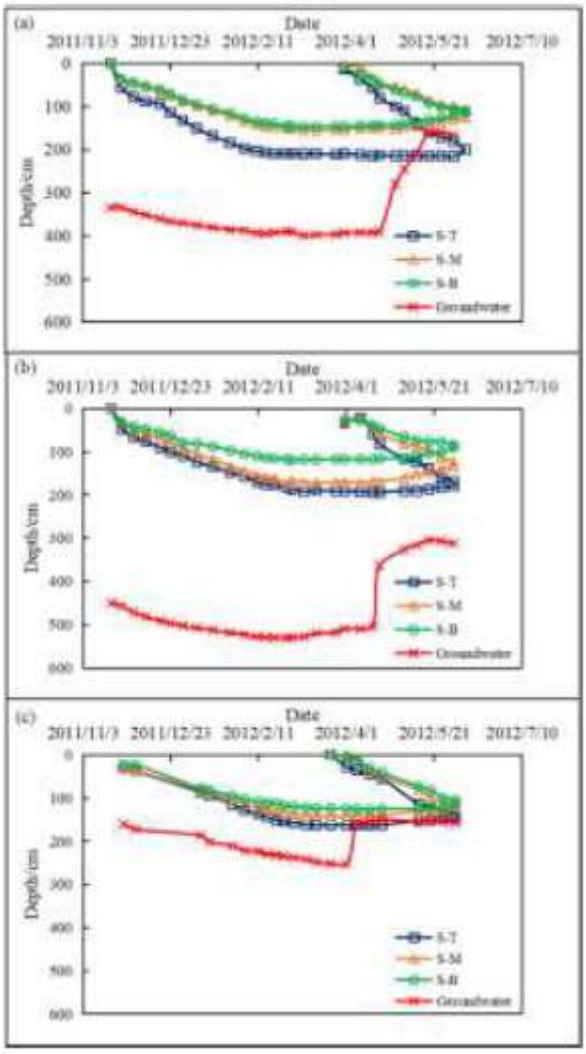

Figure 6

Soil slope - Groundwater, freeze depth monitoring curve (a: 2km test site, b: 4km test site, c: 47km test site. S: Slopes, T-top of slope, M-middle of slope, B-bottom of slope.)

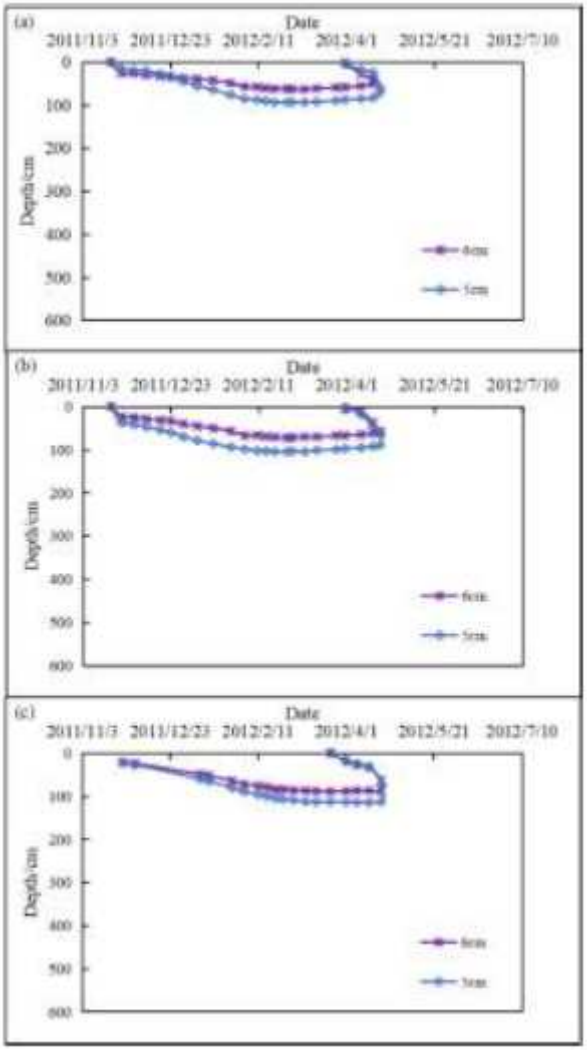

Figure 7

PB - Groundwater, freeze depth monitoring curve (a: 2km test site, b: 4km test site, c: 47km test site)

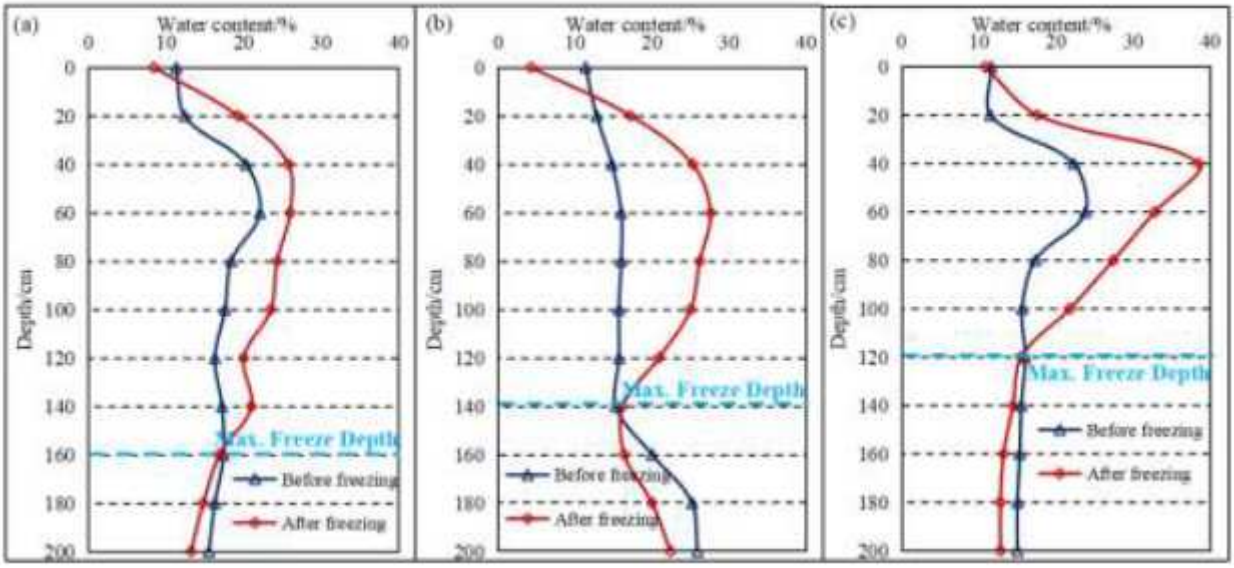

Figure 8

Moisture content change curve of the soil before and after freezing (a: Top, b: Middle, c: Bottom)

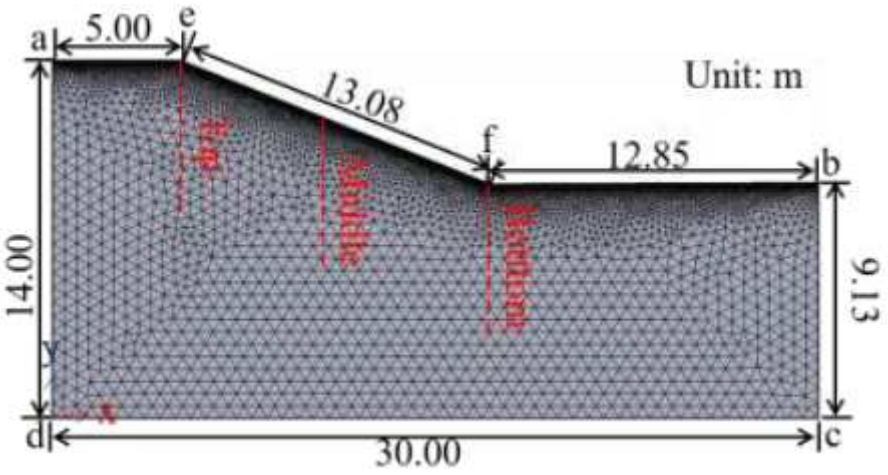

Figure 9

Numerical calculation model

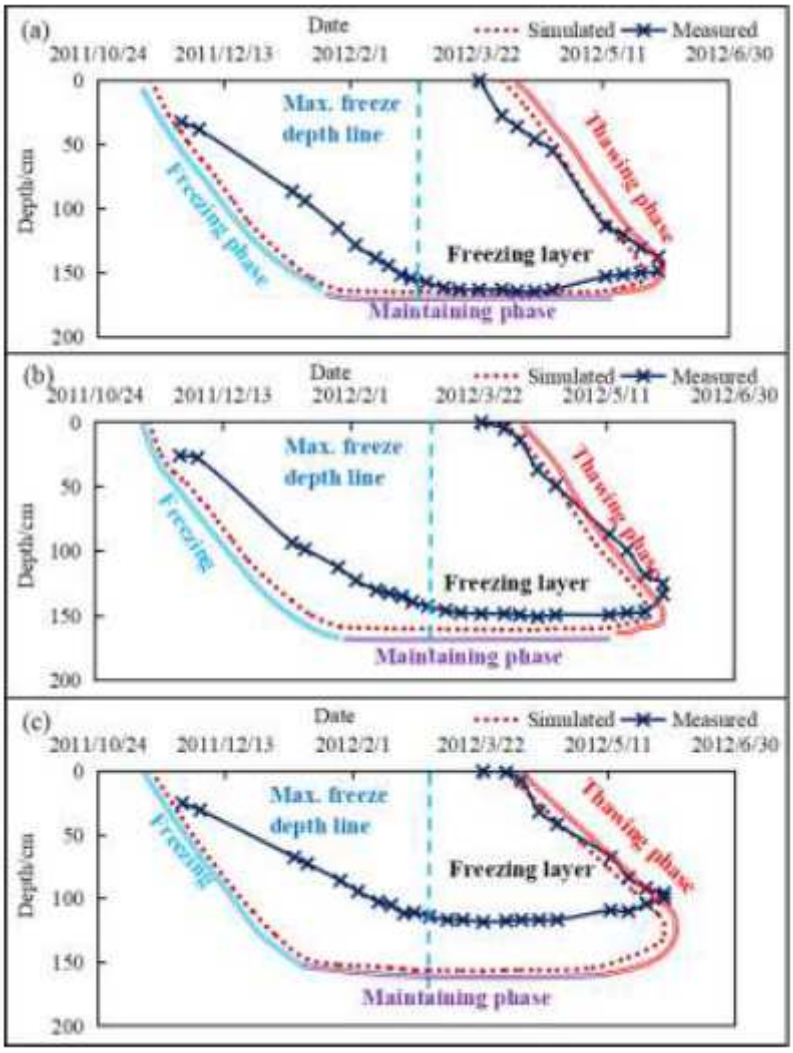

Figure 10

Freeze-thaw curves for slopes (a: Top, b: Middle, c: Bottom)

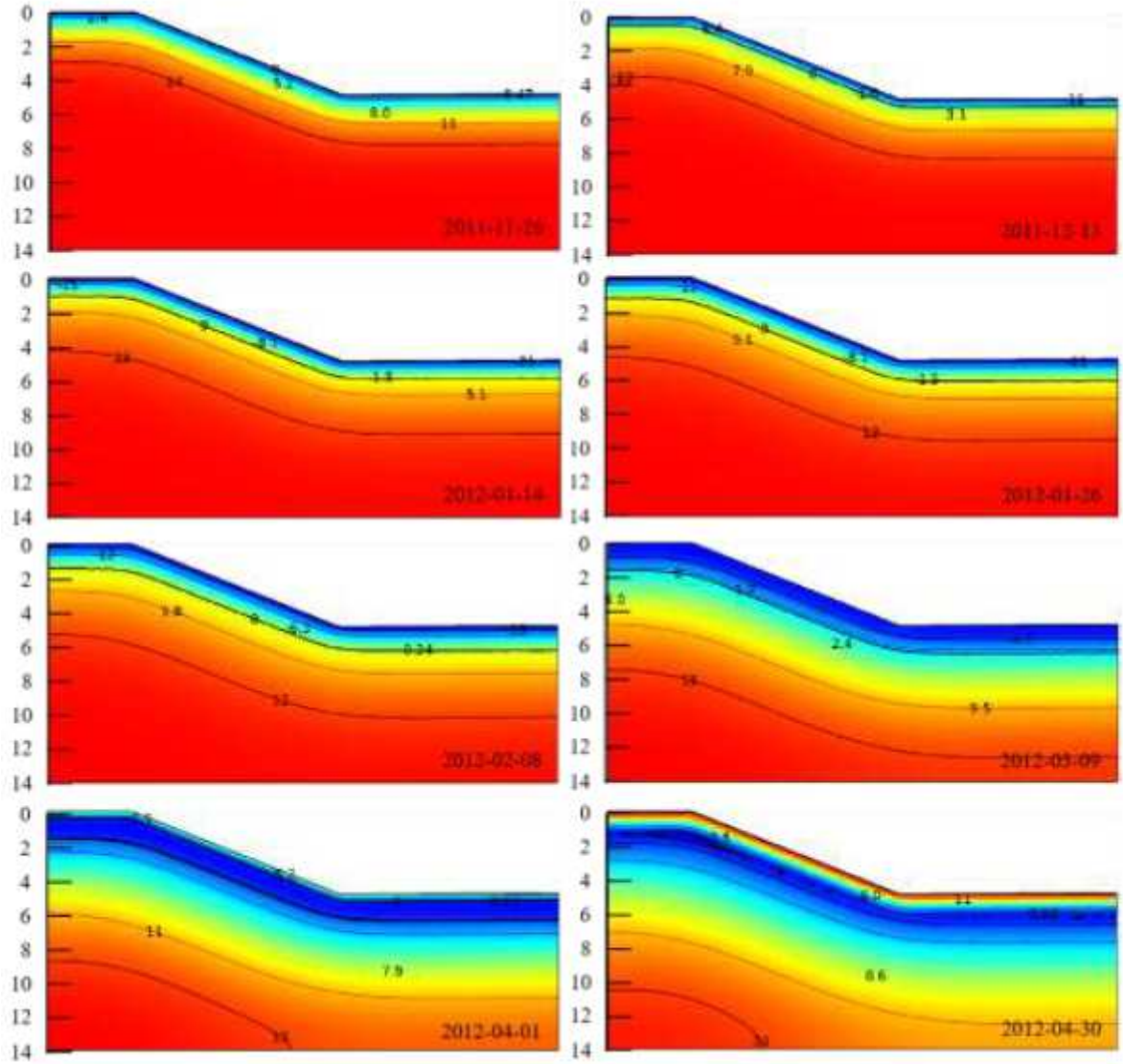

Figure 11

Temperature field distribution at different times(unit: ℃)

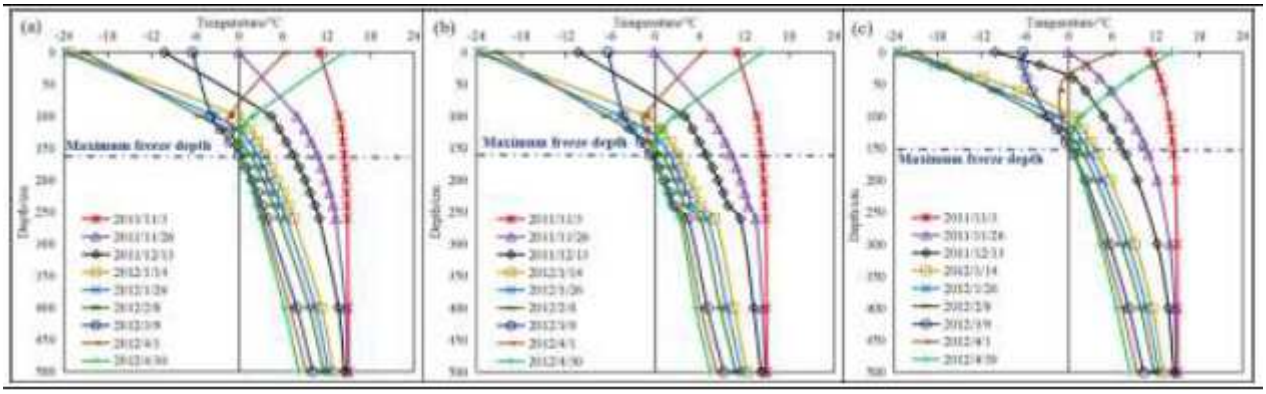

Figure 12

Temperature variation curves (a: Top, b: Middle, c: Bottom)

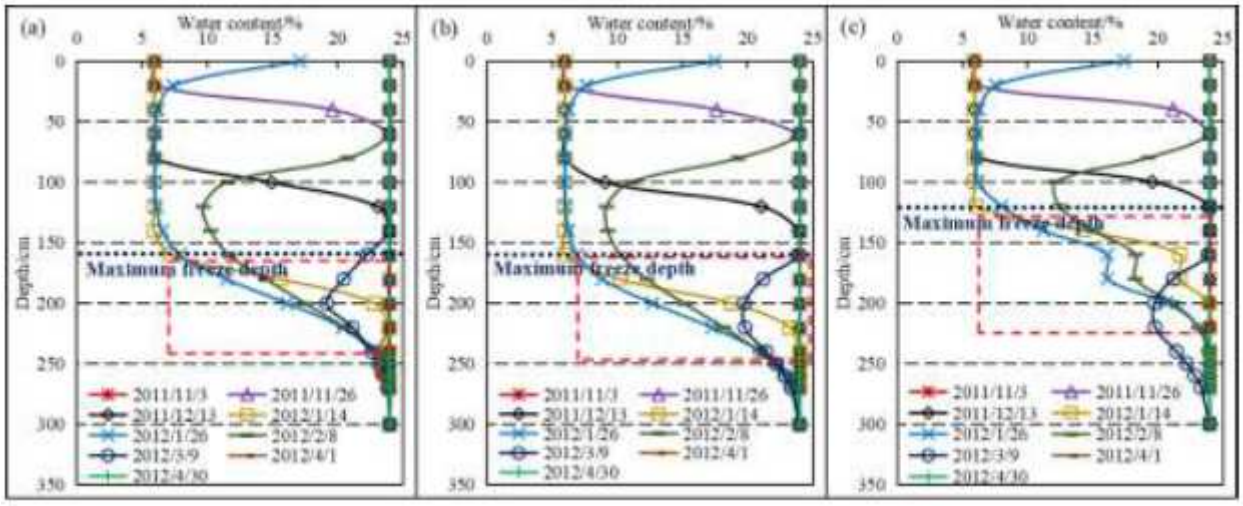

Figure 13

Water content variation curves (a: Top, b: Middle, c: Bottom)

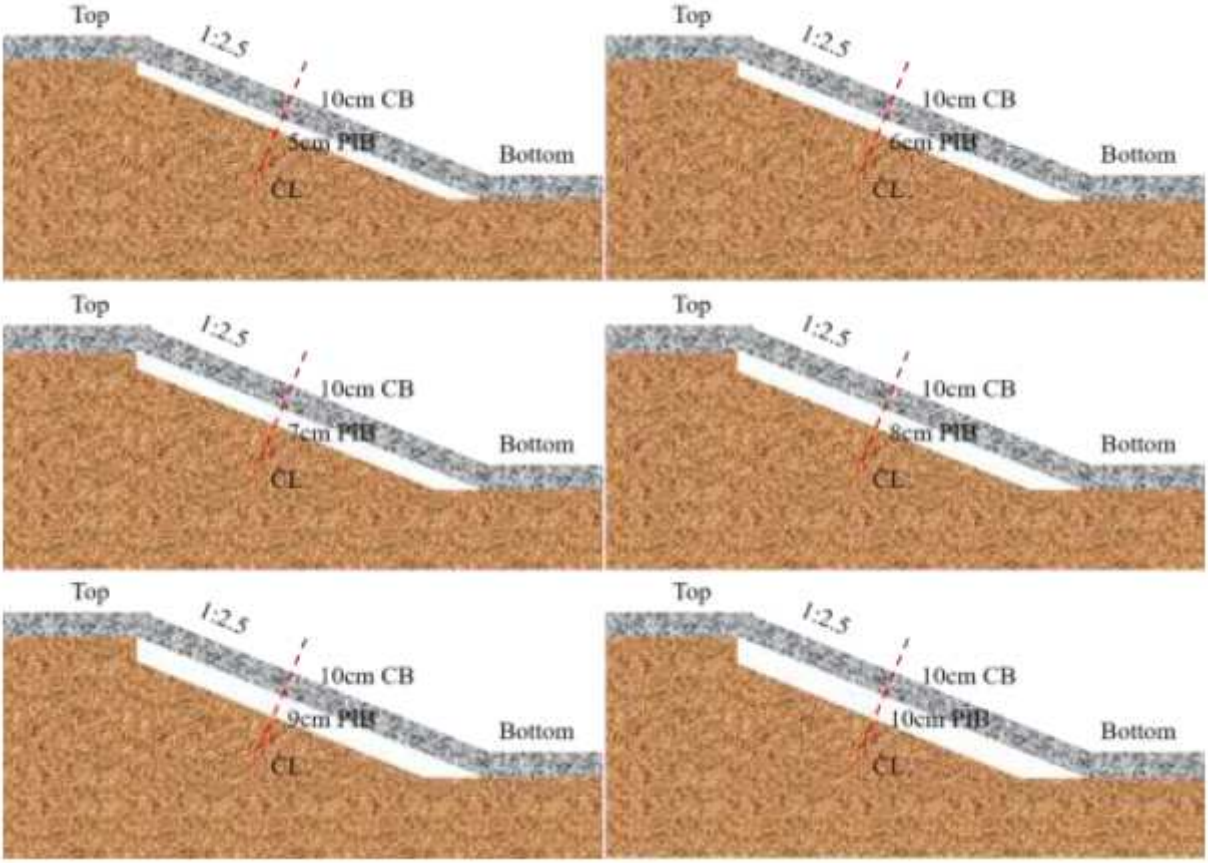

Figure 14

Anti-frost structures on the slopes of water conveyance canals in seasonal frozen regions Based on the numerical model established in this paper, the maximum freeze depth distribution can be computed. For

the convenience of modelling, a thin layer boundary condition is used instead of the insulation board solid mesh. The insulation board, as well as concrete material parameters, are shown in Table 3.

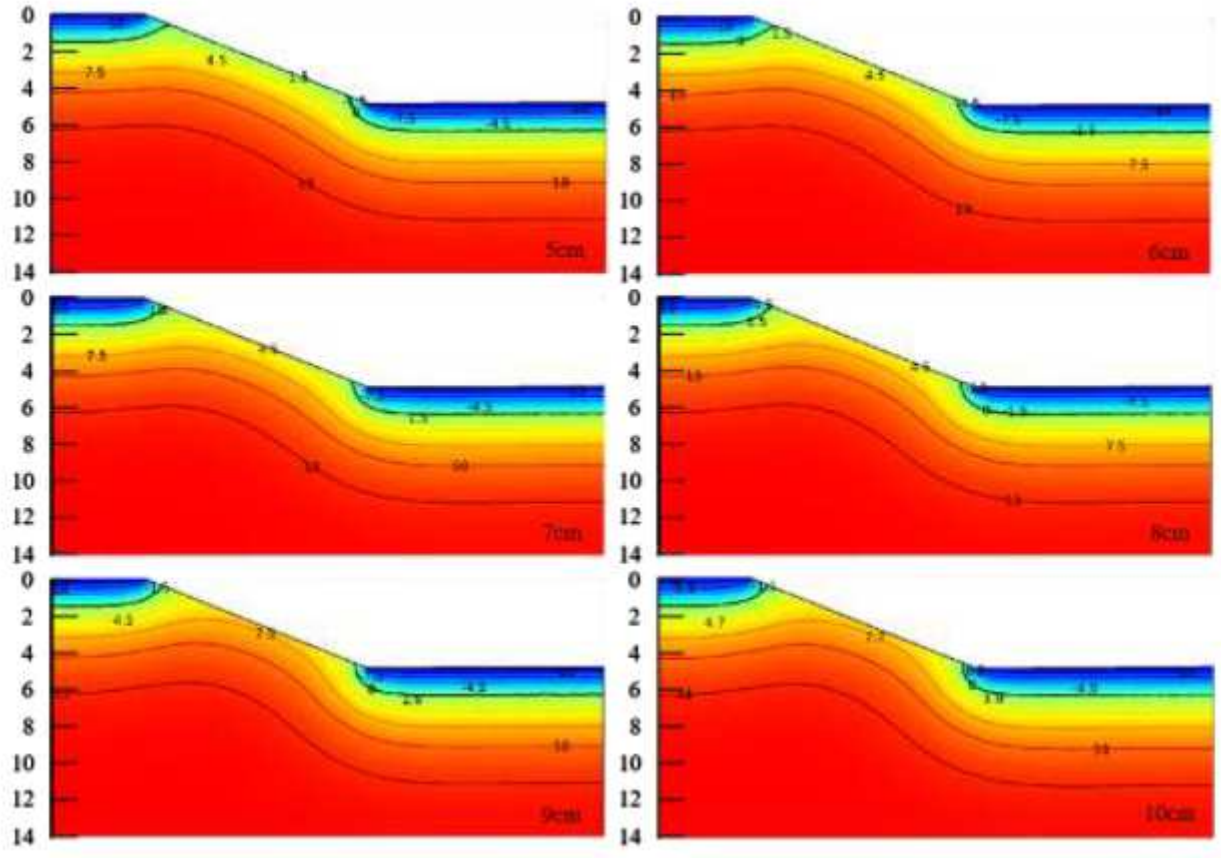

Figure 15

Temperature fields of the six anti-frost structures at maximum frost depth time

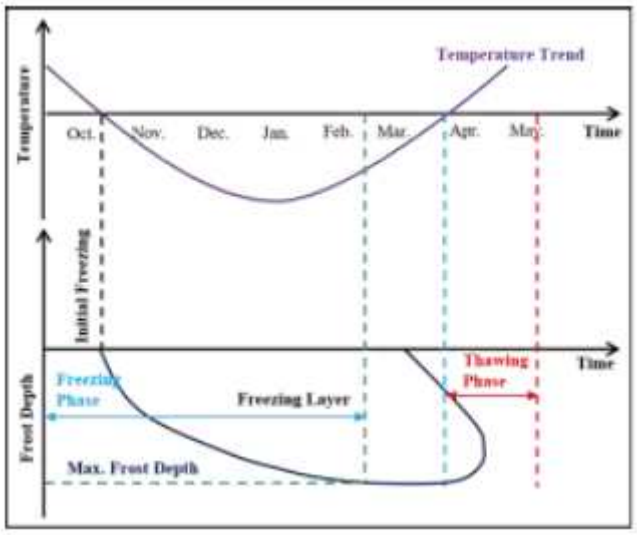

Figure 16

Frost Depth-Time Curve

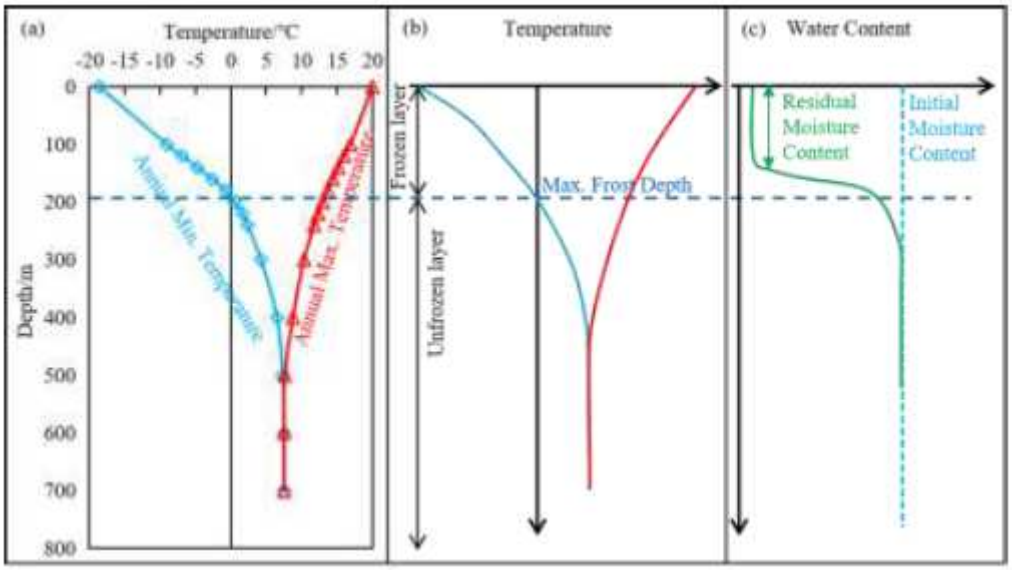

Figure 17

Characteristics of Temperature-Depth- Water content variation in the seasonal frozen regions (a: Simulated Value, b: Tempeture-Depth Trend, c: Water Content-Depth Trend)